



Contents lists available at ScienceDirect



Catalysis Today

journal homepage: www.elsevier.com/locate/cattod

Efficient production of 5-ethoxymethylfurfural from fructose by sulfonic mesostructured silica using DMSO as co-solvent

G. Morales*, M. Paniagua, J.A. Melero, J. Iglesias

Chemical and Environmental Engineering Group, ESCET, Universidad Rey Juan Carlos, C/Tulipán s/n, Móstoles, E28933 Madrid, Spain

ARTICLE INFO

Article history:

Received 13 December 2015

Received in revised form 25 February 2016

Accepted 26 February 2016

Available online xxx

Keywords:

Fructose

5-Ethoxymethyl furfural

Dimethyl sulfoxide

Response surface methodology

Sulfonic acid

Mesoporous silica

ABSTRACT

The use of sulfonic acid-functionalized heterogeneous catalysts in conjunction with the use of dimethyl sulfoxide (DMSO) as co-solvent in the catalytic transformation of fructose in ethanol to produce 5-ethoxymethyl furfural (EMF) is shown as an interesting alternative route for the production of this advanced biofuel. Arenesulfonic acid-modified SBA-15 mesostructured silica ($\text{Ar}-\text{SO}_3\text{H}-\text{SBA-15}$) has been the most active catalyst, ascribing its higher catalytic performance to the combination of excellent textural properties, acid sites surface concentration and acid strength. Noticeably, DMSO promotes the formation of EMF and HMF, reducing the extent of side reactions. Reaction conditions (temperature, catalyst loading and DMSO concentration) were optimized for $\text{Ar}-\text{SO}_3\text{H}-\text{SBA-15}$ via response surface methodology leading to a maximum EMF yield of 63.4% at 116 °C, 13.5 mol% catalyst loading based on starting fructose and 8.3 vol.% of DMSO in ethanol after 4 h of reaction. Catalyst was reused up to 4 consecutive times, without regeneration treatment, showing a slight gradual decay in activity attributed to the formation of organic deposits on the catalyst's surface.

© 2016 Elsevier B.V. All rights reserved.

1. Introduction

Diminishing fossil fuel reserves along with the need for greening of land transport, aiming to reduce air pollution, are key concerns for the present century. Such environmental objectives are driving society towards the search for new renewable energy sources for transport that may advantageously substitute fossil sources. Lignocellulosic biomass is abundant, and it has the potential to significantly displace petroleum in the production of not only fuels but also valuable chemicals, especially through the transformation of sugars coming from the hydrolysis of cellulose and hemicellulose [1]. Limitations of conventional biofuels (first generation biodiesel and bioethanol) and new trends in legislation have stimulated the search for new technologies providing energy-dense (i.e., lower oxygen content) biomass-derived fuels. Such advanced biofuels could be easily implemented in the existing hydrocarbon-based transportation infrastructure (e.g. engines, fuelling stations, distribution networks and petrochemical processes) and, importantly, not depending on edible biomass for their production.

Among the wide range of possibilities, an interesting approach is the transformation of lignocellulosic platform molecules into oxy-

genated compounds, which can be used as blend components for the reformulation of conventional fuels (gasoline and diesel), in some cases even improving certain fuel properties [2]. In this context, 5-ethoxymethylfurfural (EMF), the main representative of the 5-alkoxymethylfurfural ethers family, is considered as an excellent component for diesel-range fuels. It has relatively high energy density, similar to regular gasoline and nearly as good as diesel fuel, and significantly higher than the bioethanol, currently the most extended biofuel [3]. EMF has been evaluated admixed with commercial diesel in engine tests, leading to promising results in terms of engine performance, accompanied by a significant reduction of soot (fine particulates), and SO_x emissions [4]. Consequently, there is currently a remarkable interest in the synthesis of EMF from renewable resources such as cellulosic materials. Most of the studies in literature have been focused on the synthesis of EMF from 5-hydroxymethylfurfural (HMF). HMF is the dehydration product of biomass hexoses (mainly glucose and fructose) and can be easily etherified with ethanol by means of acid catalysis, advantageously using solid acid catalysts [5]. While relative high EMF yields can be obtained using this approach, the direct use of HMF as a precursor for the preparation of EMF is not still industrially interesting. The reason is that HMF is a very reactive molecule, difficult to isolate in good yields. Another proposed strategy is via 5-chloromethylfurfural by substitution with an alcohol. This proposal seeks to replace the OH group within the HMF molecule by

* Corresponding author.

E-mail address: gabriel.morales@urjc.es (G. Morales).

a chlorine atom, leading to 5-(chloromethyl)furfural (CMF) [6,7]. Thereafter, the nucleophilic substitution of the Cl with ethanol easily leads to the formation of EMF, giving HCl as by-product. Although high EMF yields are achievable, the presence of HCl may generate serious problems in the industrial processing. Likewise, SBA-15-supported sulphated zirconia, a bifunctional catalyst showing both Lewis and Brønsted acid sites, has also been successfully applied to HMF etherification with ethanol, demonstrating the existence of a quantitative relationship between the concentrations of each type of acid sites within the catalyst [8].

A more appealing methodology is the one-pot combination of the dehydration of cheap and renewable source such as fructose into HMF, together with the etherification into EMF using ethanol as solvent and a heterogeneous acid catalyst. Both transformations are driven by acid catalysis, being feasible to optimize the selectivity towards EMF through the proper selection of the acid catalyst and the reaction conditions. For instance, a conventional mineral acid such as sulfuric acid has been used as catalyst in this one-pot system [9]. In this work, a mechanistic study of the reaction pathway indicated that the dehydration of EMF into EL is the slowest transformation, not being the sole pathway responsible for EL formation. On the other hand, the implementation of solid acid catalysts would have several advantages over mineral acids, especially in terms of selectivity and management of the transformation. Therefore, the use of selective solid catalysts is of great interest in this transformation. In a pioneering work, Brown and co-workers evaluated the preparation of ethers of HMF, together with HMF itself and alkyl levulinates, from fructose using ion-exchange resins in non-aqueous solvents [10]. However, both the selectivity to EMF and the reaction rates were low. In a similar way, more recently, a catalyst based on silica-sulfuric acid provided 70% EMF yield at 110 °C, but still requiring excessively long reaction times [11]. In another example, Liu et al. proposed the use of a heteropolyacid-based organic-inorganic hybrid catalyst, $[MIMBS_3]PW_{12}O_{40}$, leading to high EMF yields at moderate temperatures [12]. Kraus et al. used recyclable sulfonic acid-functionalized ionic liquids (ILs), providing a biphasic system that was shown as a key factor to significantly enhance both yield and selectivity, avoiding interferences from humins-type by-products [13]. As an indication of the current relevance of the investigation on EMF production from fructose, during the last year several other heterogeneous catalytic systems have been reported: magnetic sulfonic nanoparticles ($Fe_3O_4@C-SO_3H$) [14]; acid-base bifunctional hybrid nanospheres prepared from the self-assembly of basic amino acids and phosphotungstic acid (HPA) [15]; H-USY, dealuminated H-beta zeolite, Amberlyst-15, SO_3H -SBA-15 [16].

On the other hand, during the production of EMF from fructose in ethanol using solid acid catalysts it is particularly important to prevent formed HMF from rehydrating to yield levulinic acid, reaction favoured in the presence of strong acid catalysts even in the presence of very small amounts of water. Such consumption of HMF limits the formation of EMF, while increases the production of ethyl levulinate (EL) from the esterification of levulinic acid in ethanol medium (Scheme 1). Thus, though EL might also be considered a target fuel additive [17], if the desired product is EMF, the rehydration must be prevented. In this sense, many authors have previously reported on the use of an aprotic organic solvent such as dimethylsulfoxide (DMSO) in the dehydration of hexoses to 5-hydroxymethylfurfural [18–22]. DMSO can stabilize the formed HMF, significantly reducing undesired side-reactions leading to the formation of humins, as well as levulinic acid. Furthermore, DMSO can play an active role in the reaction, since at high temperature it has the effect of modifying the tautomeric forms of fructose, increasing the presence of furanose versus pyranose forms, making easier the dehydration into HMF, precursor to EMF [23]. A recent work by Wang et al. demonstrated the benefits of using DMSO in

the production of EMF from fructose in ethanol using a commercial homogeneous heteropolyacid HPW catalyst [24]. On the other hand, several authors have brought the attention on the main drawback of using DMSO in HMF production, which is the difficulty of the separation of both chemicals by conventional processes such as distillation, due to the high boiling point of HMF and its sensitivity to high temperatures. However, a recent work on the room temperature separation of HMF from DMSO by selective adsorption on porous activated carbons, have provided a cost-effective recovery process [25], avoiding the disadvantages of high temperature separation.

In this context, sulfonic acid-functionalized mesostructured materials have demonstrated an excellent behaviour in the catalytic transformation of biomass-derived compounds into added-value products, such as biodiesel from non-conventional feedstocks [26], glycerol derivatives from crude glycerin [27,28], HMF from glucose [22], levulinates from levulinic acid [29], etc. These materials, featured by high surface area, large uniform pores, high thermal stability, and the capability to control the surface hydrophilic/hydrophobic balance as well as the strength and concentration of acid sites, appear as promising catalysts for this sort of acid-catalyzed reactions. More broadly, solid acids with SO_3H acid sites and tunable surface properties appear to have a large potential in the valorization of biomass [30].

In this contribution, we have studied the catalytic performance of several sulfonic-containing heterogeneous acid catalysts in the conversion of fructose to EMF, investigating the effect of using DMSO as co-solvent, followed by a multivariate analysis to assess the optimal reaction conditions – catalyst loading, temperature and DMSO content – to maximize the production of EMF over these catalysts.

2. Experimental

2.1. Materials

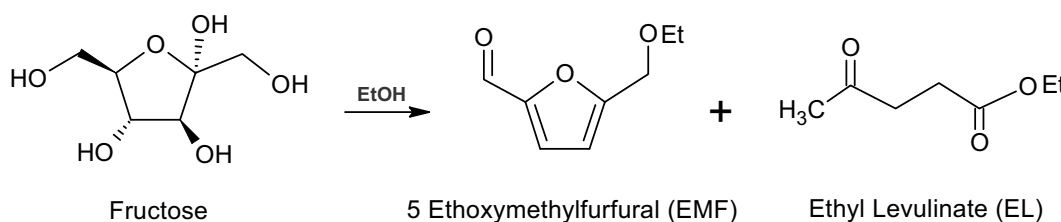
Fructose (99% purity), 5-(hydroxymethyl) furfural (HMF, 99% purity), 5-ethoxymethylfurfural (EMF, 97% purity) and ethyl levulinate (EL, 99% purity) were purchased from Sigma-Aldrich. Ethanol (99.9% purity) and dimethyl sulfoxide (DMSO, 99.8% purity) were obtained from Scharlab. Decane (99% purity) was acquired from Across Organics. All the chemicals were used as received without previous purification.

2.2. Catalysts

Several sulfonic acid-containing heterogeneous catalysts have been evaluated in the dehydration of fructose. Propylsulfonic acid and arenesulfonic acid functionalized mesostructured silicas ($Pr-SO_3H$ -SBA-15 and $Ar-SO_3H$ -SBA-15, respectively) were synthesized following previously reported procedures [31,32]. As reference catalysts, commercial acid catalysts were also evaluated in this work. Acidic macroporous resin, Amberlyst-15, and a homogeneous catalyst, *p*-toluenesulfonic acid (PTSA), were supplied by Sigma-Aldrich.

2.3. Catalysts characterization

The textural properties of the sulfonic acid-modified mesostructured silicas were obtained by means of nitrogen adsorption-desorption isotherms recorded at 77 K using a Micromeritics TRISTAR 3000 system. Pores sizes distributions were calculated using the BJH method using the KJS correction, and total pore volume was taken at $P/P_0 = 0.975$. Structural characterization was performed by X-ray powder diffraction (XRD) patterns, which were acquired on a PHILIPS X'PERT diffractometer using the $Cu K\alpha$ line.



Scheme 1. Main products of the acid-catalyzed transformation of fructose in ethanol.

Data were recorded from 0.6 to 5° (2θ) with a resolution of 0.02°. Acid capacity was measured by the determination of cationic-exchange capacity using sodium as the cationic-exchange agent. Thermogravimetric analyses (TGA) were performed in a SDT 2960 Simultaneous DSC-TGA, from TA Instruments with an air flow rate of 100 mL/min and a heating ramp of 5 °C/min. **Table 1** summarizes the most relevant physicochemical properties recorded for the acid catalysts tested in this work.

2.4. Catalytic tests

Reaction runs were performed in ACE pressure glass reactors immersed in an oil bath under strict temperature control. After a specific reaction time, tube reactor was removed from the oil bath and rapidly cooled down to room temperature. For catalysts screening, fructose dehydrations were performed in ethanol up to 8 h at 110 °C, adding the appropriate amount of each catalyst to achieve a constant acid sites loading of 0.05 mmol H⁺. For the optimization of reaction conditions, the reaction variables investigated through a multivariate analysis were: catalyst loading (5–15% of acid sites based on fructose, mol/mol), temperature (90–130 °C), and DMSO loading (5–10 vol.%). Typically, the composition of the reaction mixture was 0.18 g of fructose (1 mmol), 0.05 g of decane as internal standard and 5 mL of solvent (mixture of ethanol and DMSO), and the respective mass of catalyst. In the optimization study reaction time was fixed at 4 h. Thereafter, under the optimized reaction conditions, a kinetic study was carried out in the range 0–24 h.

2.5. Product analysis

Reaction samples were analysed combining gas and liquid chromatography, using a Varian 3900 gas chromatograph and a Varian ProStar HPLC chromatograph, respectively. Fructose was quantified by HPLC using a Hi-Plex H⁺ column and a refractive index detector (Varian 356-LC). 0.005 M aqueous sulfuric acid was used as eluent, using a flow rate of 0.6 mL/min keeping the column temperature at 60 °C. Reaction products detected by GC included HMF, EMF and EL. In the experiments without DMSO, GC analysis was performed using a ZB-WAX Plus column and a FID detector. In the experiments with DMSO, since EL and DMSO eluted together at the same retention time, a second GC column was required. In this case, a VARIAN CP-8944 column and a FID detector was used to quantify EL. Catalytic results are shown either in terms of absolute conversion of fructose or in terms of yields towards the different products (Y_i).

Product quantification was based on a previous calibration of the analysis unit with standard stock solutions of pure commercially available chemicals.

$$X_{\text{fructose}} = \frac{\text{Reacted mol of fructose}}{\text{Initial mol of fructose}} \times 100$$

$$Y_i = \frac{\text{Formed mol of } i}{\text{Initial mol of fructose}} \times 100$$

3. Results and discussion

3.1. Catalysts screening

Fructose was converted into EMF over different sulfonic acid-based catalysts in ethanol in order to identify the catalyst offering the optimal performance for this transformation. Catalysts assayed in this work have included propyl- and arene-sulfonic acid-modified SBA-15 mesoporous silicas, which have been shown previously as very active catalysts in other acid-catalyzed reactions [33]. These synthesized catalysts were benchmarked with a sulfonic macroporous resin, commercially available and conventionally used in many acid-catalyzed processes, such as Amberlyst-15; as well as a homogeneous sulfonic acid, *p*-toluenesulfonic acid (PTSA). The nature of the active sulfonic acid sites is similar for PTSA, Amberlyst-15 and Ar-SO₃H-SBA-15, all of them presenting an aromatic ring directly attached to the SO₃H group. The electron-withdrawing effect introduced by said aromatic ring acts as an acid strength enhancer, resulting in stronger sulfonic sites [32]. On the other hand, the alkyl nature of the tethering moiety in the propyl-sulfonic acid-modified SBA-15 silica (Pr-SO₃H-SBA-15) results in a lower acid strength. A blank reaction experiment, performed in the absence of catalyst, was also performed, showing negligible production of EMF. **Fig. 1** depicts the results of the catalyst screening carried out under arbitrarily selected reaction conditions, based on preliminary experiments and literature. For a better comparison, catalysts mass loadings were adjusted as a function of their acid capacities (**Table 1**), so that a constant acid sites molar loading was achieved (0.05 mmol H⁺).

As shown in **Fig. 1**, after 8 h at 110 °C all the catalysts provided 100% fructose conversion, with the exception of Amberlyst-15. At this temperature, the reaction can be considered fast, especially with the homogeneous PTSA catalyst, rapidly leading to the transformation of fructose into HMF as an intermediate that subsequently evolves to EMF and EL. The appearance of ethyl levulinate becomes more significant at higher reaction times. It must be

Table 1

Physicochemical properties of SO₃H-based catalysts.

Catalyst	BET area (m ² /g)	Pore volume (cm ³ /g)	Pore Size(Å)	Acid capacity(meq H ⁺ /g)	SO ₃ H surface concentration(μeqH ⁺ /m ²)	T limit(°C)
Amberlyst-15 ^a	45	0.40	300	4.70	104	120
PTSA	–	–	–	5.80	–	–
Pr-SO ₃ H-SBA-15	721	1.18	81	1.03	1.43	>200
Ar-SO ₃ H-SBA-15	712	0.97	92	0.92	1.29	>200

^a Properties provided by the suppliers or experimentally determined.

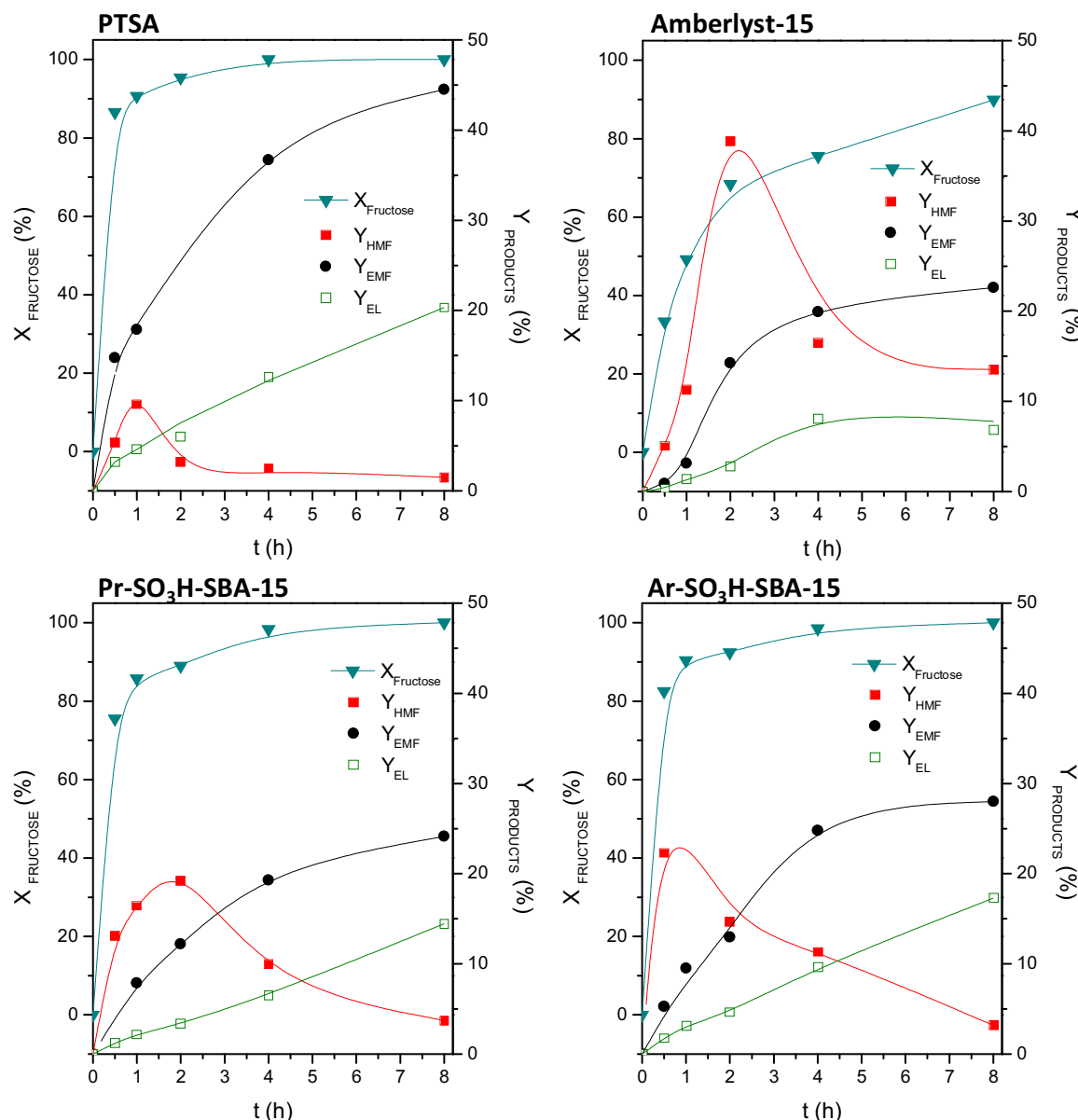


Fig. 1. Fructose conversion (left axes) and yields to HMF, EMF and EL (right axes) in the transformation of fructose to EMF in ethanol using different sulfonic acid catalyst. Reaction conditions: 1 mmol fructose, 0.05 mmol H⁺ catalyst, 5 mL ethanol, 110 °C.

noted that, in order to close reaction mass balance, there must be other unidentified products, either degradation by-products (humin-type) or intermediates such as ethyl-fructoside. This set of data confirms previously reported main reaction mechanism including the steps of fructose dehydration into HMF, etherification of HMF to EMF and rehydration of EMF into EL, the final product. As expected, due to its homogeneous nature, PTSA is the most active catalyst, providing the highest production of EMF (maximum yield to EMF of 49% at 8 h). However, this high EMF production is accompanied by a sustained production of EL, reaching over 20% yield at 8 h. On the other hand, the performance of the three solid acid catalysts can be correlated to their textural properties as well as to the availability and strength of their acid sites (Table 1). In this case, the commercial acid resin Amberlyst-15 has the lowest specific surface, thus leading to a poor accessibility to the acid sites. Furthermore, surface acid sites concentration is extraordinarily elevated for this catalyst (104 μeqH⁺/m², Table 1). This is most likely strongly affecting the local hydrophilicity of the solid surface [34], which is a key parameter controlling the diffusion of

bulky substrates such as monosaccharides and their derivatives. Mesostructured catalysts, on the contrary, display high BET surface areas with a much more moderate surface acid concentration. In this way, Ar-SO₃H-SBA-15 led to a higher EMF yield at 8 h than Amberlyst-15, 29% vs. 22%, respectively. Additionally, the steps of fructose dehydration and HMF etherification occur faster over this catalyst. On the contrary, Pr-SO₃H-SBA-15 catalyst displays a similar behaviour though reaching lower values of EMF and EL final yields. Since the support matrix (silica mesostructured), the acid capacity and the surface concentration are very similar, such a lower catalytic performance as compared to Ar-SO₃H-SBA-15 can be attributed to the lower inherent acid strength of alkyl- vs. arene-sulfonic acid sites. Therefore, among the heterogeneous catalysts, the mesostructured Ar-SO₃H-SBA-15 shows the best catalytic performance due to the combination of a suitable acid strength and excellent textural properties, and it was the selected catalysts for the following optimization of the reaction.

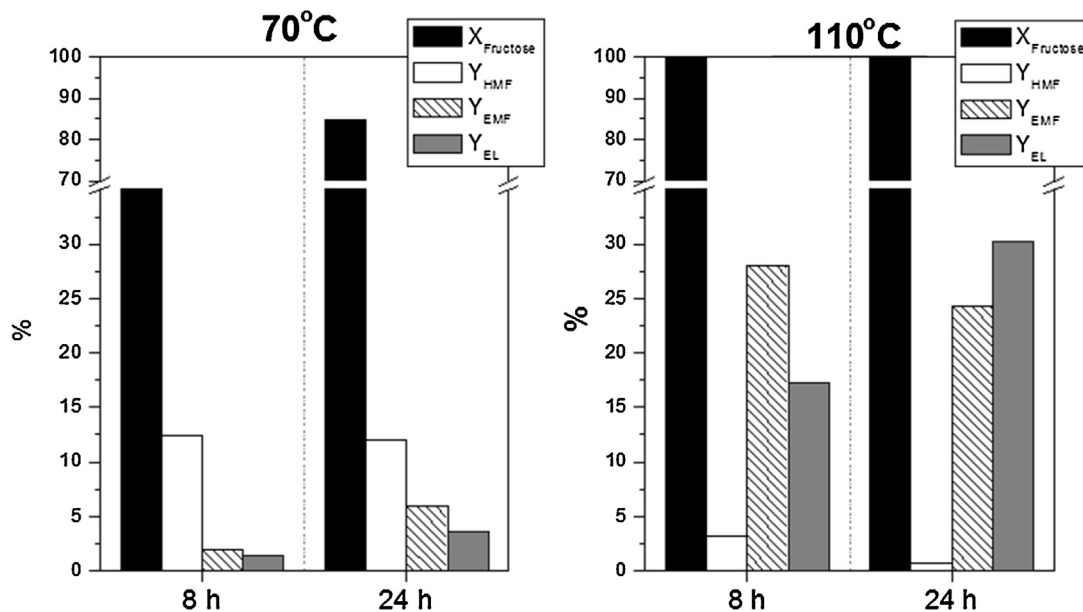


Fig. 2. Effect of reaction temperature and time in the transformation of fructose in ethanol to give HMF, EMF and EL over Ar-SO₃H-SBA-15 catalyst. Reaction conditions: 1 mmol fructose, 0.05 mmol H⁺, 5 mL ethanol.

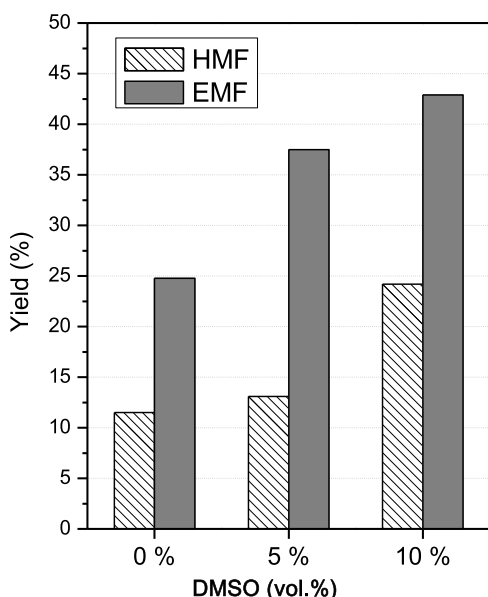


Fig. 3. Effect of the addition of DMSO to the reaction medium. Catalyst, Ar-SO₃H-SBA-15. Reaction conditions: 110 °C, 4 h, 1 mmol fructose, 0.05 mmol H⁺, 5 mL total reaction volume.

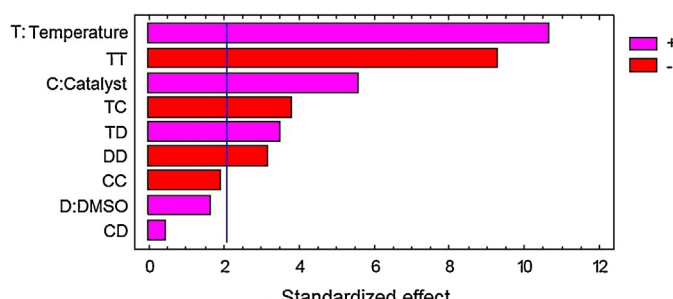


Fig. 4. Standardized Pareto chart for yield to EMF.

3.2. Optimization of reaction conditions with Ar-SO₃H-SBA-15

From the above catalysts screening, Ar-SO₃H-SBA-15 was selected as the best solid catalyst to further analyse the reaction variables. The objective was to maximize EMF yield through the proper selection of the reaction conditions. Significant variables were first identified. Fig. 2 includes the results of fructose conversion and yield to the main products (HMF, EMF and EL) at two different temperatures, 70° and 110 °C, after 8 h and 24 h. As shown, temperature dramatically affects the catalytic performance, especially in terms of yields to EMF and EL. Products distribution is clearly different at 70 °C, favouring the formation of HMF over the ether and/or the ester. However, as occurred over Amberlyst-15 (Fig. 1), the conversion of fructose is still high at low temperature. This indicates different activation energies for the dehydration of fructose into HMF and the subsequent transformations with ethanol. In order to maximize EMF temperatures higher than 70 °C must be used. Regarding the effect of reaction time, longer reaction times clearly favour the formation of ethyl levulinate, which eventually becomes the major product at 110 °C. As a reaction intermediate, yield to EMF tends to decrease slowly at longer times. Therefore, selection of reaction time is also important to ensure maximum EMF production, while keeping the formation of EL as low as possible. From Figs. 1 and 2, for the catalyst Ar-SBA-15-SO₃H at 110 °C, an adequate reaction time around 4 h can be inferred. On the other hand, a preliminary set of experiments aiming to analyse the benefits of using dimethylsulfoxide as co-solvent was performed (Fig. 3). EMF yield is clearly enhanced even by the presence of 5 vol.% of DMSO, and increasing the concentration up to 10 vol% keeps enhancing the production of EMF. As shown, the yield towards HMF is also increased, though in a lesser degree than EMF.

In conclusion, reaction temperature and DMSO loading appear to be most influential variables in this system. On the other hand, catalyst loading is usually a key parameter in such catalytic processes. Furthermore, because of the presence of side reactions, crossed interactions between variables can be expected. Therefore, in order to simultaneously analyse the effect of these three main reaction variables, i.e. temperature, catalyst loading and DMSO concentration, an experimental design methodology was proposed [35]. Particularly, a 3³ factorial experimental design, with three dif-

Table 2

Experiments matrix and experimental results for the transformation of fructose in ethanol-DMSO over arenesulfonic acid functionalized mesostructured silica, Ar-SO₃H-SBA-15. Reaction time 4 h.

Run	T (°C) (X ₁)	C (%) (X ₂)	D (%) (X ₃)	I _T	I _C	I _D	Y _{HMF} (%)	Y _{EMF} (%)
1	90	5	5	-1	-1	0	25.5	14.2
2	110	5	5	0	-1	0	13.1	37.5
3	130	5	5	1	-1	0	0.7	36.7
4	90	10	5	-1	0	0	22.4	24.3
5	110	10	5	0	0	0	4.0	54.0
6	130	10	5	1	0	0	0.3	40.0
7	90	15	5	-1	1	0	21.8	34.6
8	110	15	5	0	1	0	1.5	61.4
9	130	15	5	1	1	0	0.4	30.9
10	110	10	7.5	0	0	0	6.5	56.2
11	110	10	7.5	0	0	0	8.7	61.4
12	110	10	7.5	0	0	0	8.2	57.1
13	90	5	7.5	-1	-1	0	24.8	8.5
14	110	5	7.5	0	-1	0	49.6	49.6
15	130	5	7.5	1	-1	0	1.6	54.7
16	90	10	7.5	-1	0	0	42.6	28.3
17	110	10	7.5	0	0	0	10.7	62.9
18	130	10	7.5	1	0	0	0.7	57.9
19	90	15	7.5	-1	1	0	29.1	31.4
20	110	15	7.5	0	1	0	3.4	63.8
21	130	15	7.5	1	1	0	0.5	49.5
22	90	5	10	-1	-1	1	37.8	11.0
23	110	5	10	0	-1	1	24.2	42.9
24	130	5	10	1	-1	1	4.3	44.2
25	90	10	10	-1	0	1	32.3	18.3
26	110	10	10	0	0	1	11.2	50.3
27	130	10	10	1	0	1	1.3	56.8
28	90	15	10	-1	1	1	36.4	34.4
29	110	15	10	0	1	1	7.8	53.2
30	130	15	10	1	1	1	1.1	56.9

Note: T, temperature; C, catalyst loading (mol% of acid sites based on fructose); D, DMSO loading (vol.% based on ethanol); I, coded value; Y_{HMF}, yield to 5-hydroxymethylfurfural; Y_{EMF}, yield to 5-ethoxymethylfurfural. Columns 2–4 represent the factor levels on a natural scale whereas columns 5–7 represent the 0 and ±1 encoded factor levels on a dimensionless scale.

ferent levels for each of the three factors, was carried out. Selection of the levels was based on the above previous results (Figs. 1–3). The lower and upper levels of the experimental factors were: 90–130 °C for the temperature, 5–15 mol% of acid sites based on fructose for the catalyst loading (equivalent to 0.05–0.15 mmol H⁺ in the reaction medium), and 5–10 vol.% based on ethanol for DMSO loading. Central point experiment (110 °C, 0.10 mmol H⁺, 7.5 vol.% DMSO) was repeated three times in order to determine the variability of the results and assess the experimental error. The selected responses were the yields towards the most relevant products, 5-hydroxymethylfurfural (Y_{HMF}) and 5-ethoxymethylfurfural (Y_{EMF}). Fructose conversion was practically total for all the experiments, whereas yield to ethyl levulinate was not determined for every run due to the complexity of analysis in the presence of DMSO (see Section 2). Nevertheless, from the analysed samples, yield to EL showed low variability within the experimental range. Optimization of the reaction variables targeted the maximization of the yield to EMF. The standard experiments matrix for the design is shown in Table 2. Experiments were run randomly to minimize errors due to pos-

sible systematic trends in the variables. Table 2 also includes the results of the yields to HMF and EMF.

The analysis of experimental data was performed according to response surface methodology using a second-order polynomial equation:

$$Y = \beta_0 + \sum_{i=1}^3 \beta_i \cdot X_i + \sum_{i=1}^3 \beta_{ii} \cdot X_i^2 + \sum_{i=1}^3 \beta_{ij} \cdot X_i \cdot X_j$$

where Y is each response (yield to HMF, yield to EMF, mol%) and β_0 , β_i , β_{ii} and β_{ij} are the regression coefficients of intercept, linear, quadratic and binary interactions, respectively. X_i and X_j are the independent factors, temperature, catalyst loading and DMSO concentration. To confirm the parameter estimation and for the sake of the model fitting, an estimation of the statistical error was performed. Eqs. (1)–(4) were obtained by multiple regression analysis using the software Statgraphics (Table 3). The statistical model was obtained from encoded levels giving the real influence of each variable on the process, and the technological model was obtained from the real values. Consequently, the influence of the variables on the

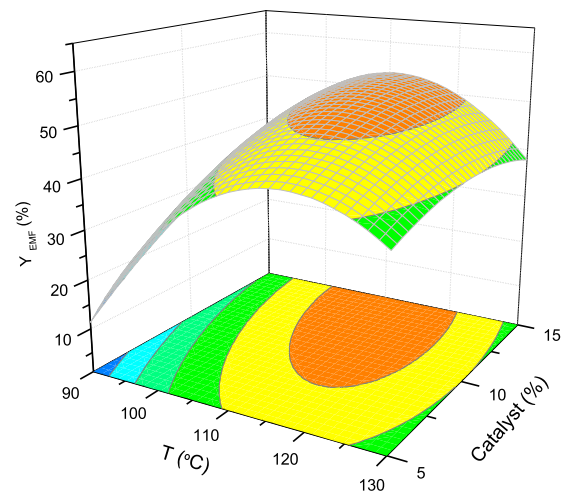
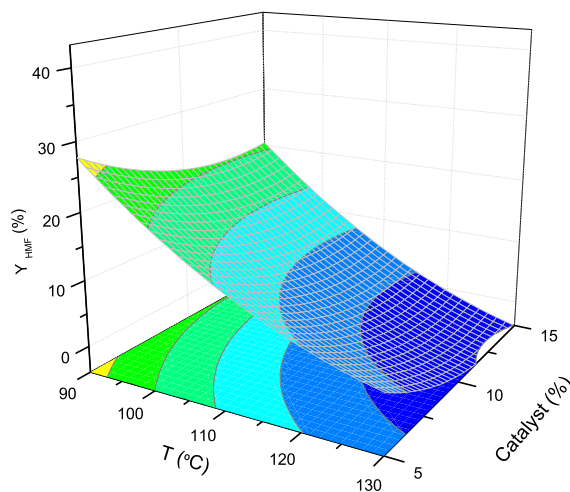
Table 3

Predictive equations obtained by response surface methodology.

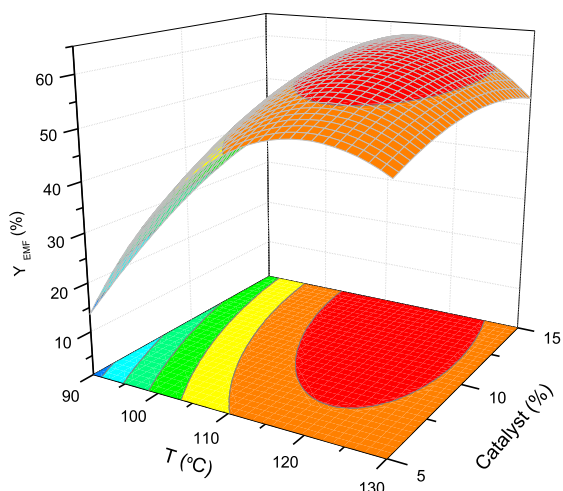
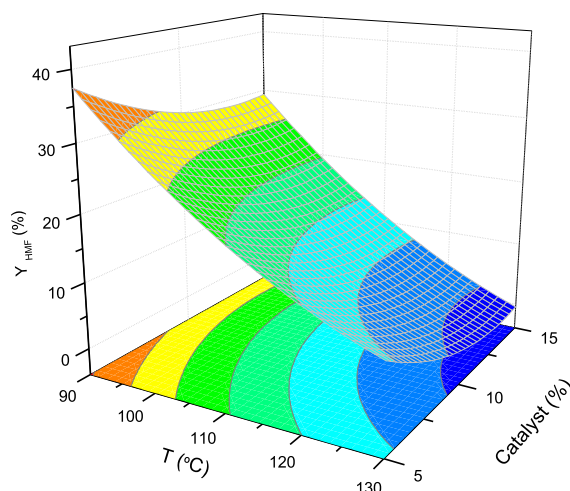
Equation	R ²
Statistical models	
$Y_{HMF} = 12.2417 - 14.5444 \cdot I_T - 4.42222 \cdot I_C + 3.70556 \cdot I_D + 3.29167 \cdot I_T^2 - 0.316667 \cdot I_T \cdot I_C - 2.625 \cdot I_T \cdot I_D + 3.29167 \cdot I_C^2 - 0.45 \cdot I_C \cdot I_D - 2.95833 \cdot I_D^2$	(1) 0.7537
$Y_{EMF} = 58.9896 + 12.3667 \cdot I_T + 6.48889 \cdot I_C + 1.91111 \cdot I_D - 17.4479 \cdot I_T^2 - 5.41667 \cdot I_T \cdot I_C + 4.975 \cdot I_T \cdot I_D - 3.64792 \cdot I_C^2 + 0.658333 \cdot I_C \cdot I_D - 5.94792 \cdot I_D^2$	(2) 0.9374
Technological models	
$Y_{HMF} = 126.772 - 2.11848 \cdot T - 2.88208 \cdot C + 14.7447 \cdot D + 0.00825661 \cdot T^2 - 0.00317583 \cdot T \cdot C - 0.052505 \cdot T \cdot D + 0.130919 \cdot C^2 - 0.03598 \cdot C \cdot D - 0.475203 \cdot D^2$	(3) 0.7537
$Y_{EMF} = -597.705 + 10,0184 \cdot T + 9.78487 \cdot C + 3.57358 \cdot D - 0.0436582 \cdot T^2 - 0.0541383 \cdot T \cdot C + 0.0994733 \cdot T \cdot D - 0.146244 \cdot C^2 + 0.0527467 \cdot C \cdot D - 0.951857 \cdot D^2$	(4) 0.9374

Note: I_T, coded value for temperature; I_C, coded value for catalyst loading; I_D, coded value for DMSO loading; Y_{HMF}, yield to 5-hydroxymethylfurfural; Y_{EMF}, yield to 5-ethoxymethylfurfural. The models include only the significant terms.

DMSO = 5%



DMSO = 7.5%



DMSO = 10%

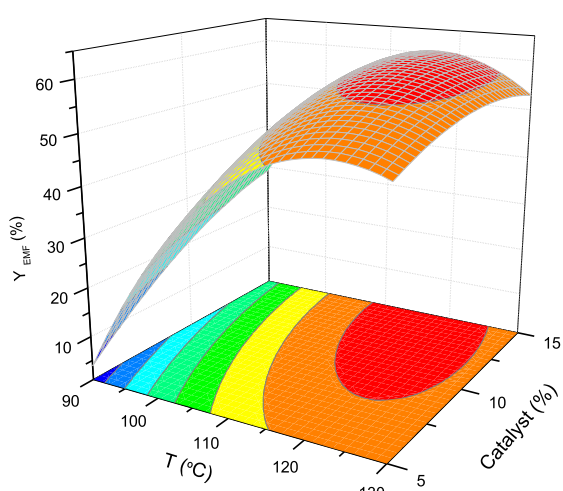
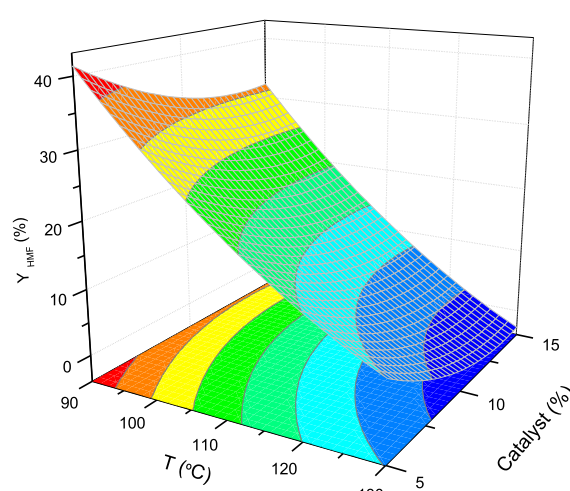


Fig. 5. Response surfaces for yield to EMF and HMF predicted by the models for the three different levels of DMSO loading. Catalyst, Ar-SO₃H-SBA-15; time, 4 h.

responses is discussed using the statistical models shown in Eqs. (1) and (2) (Table 3).

In the case of the yield to HMF (Eq. (1)), statistical analysis within the studied experimental range identifies the temperature as the most influential factor with a negative effect. In addition, the effect

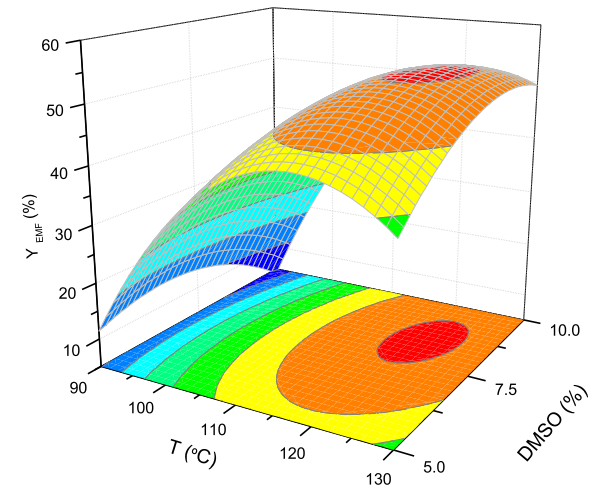
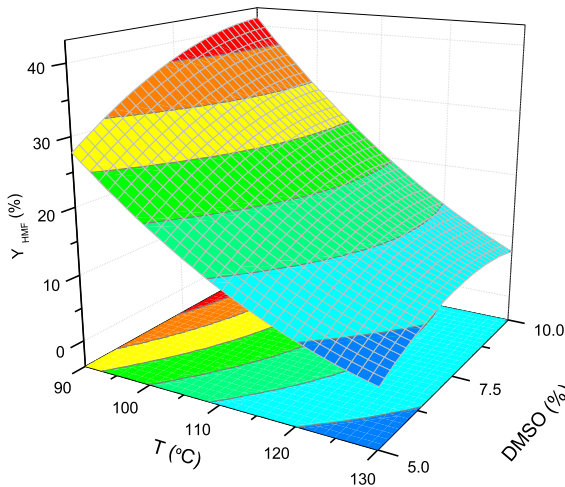
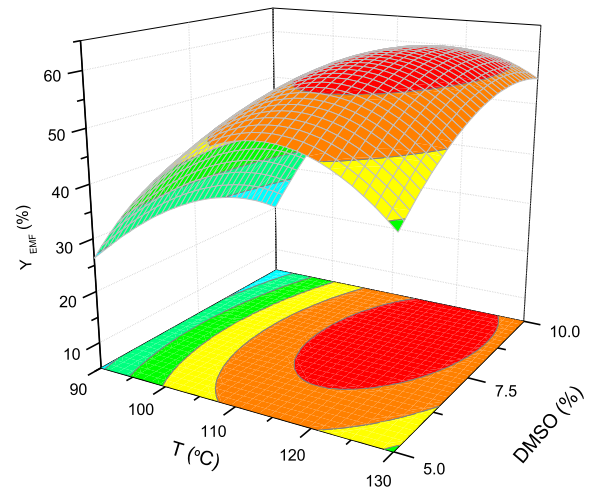
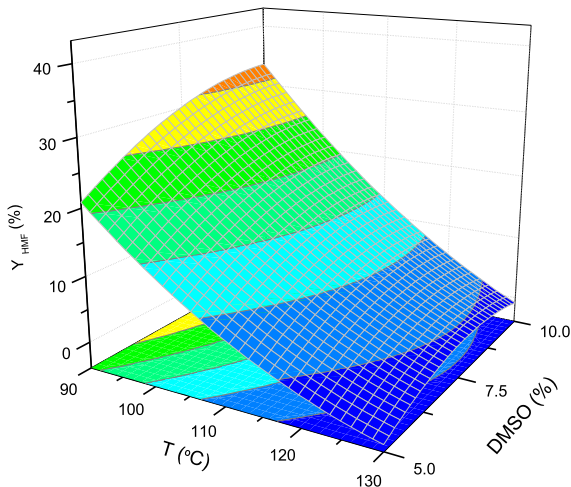
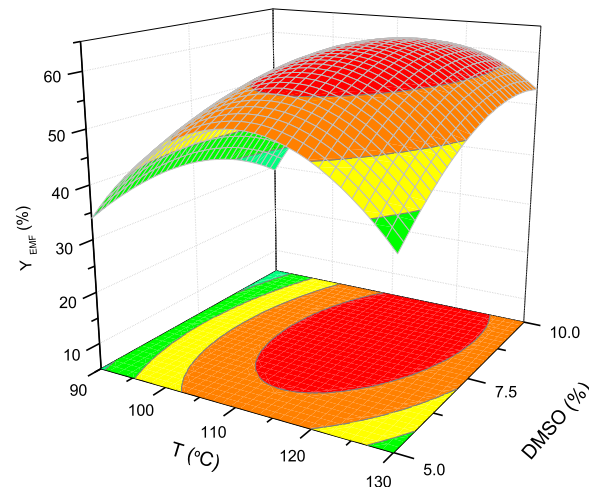
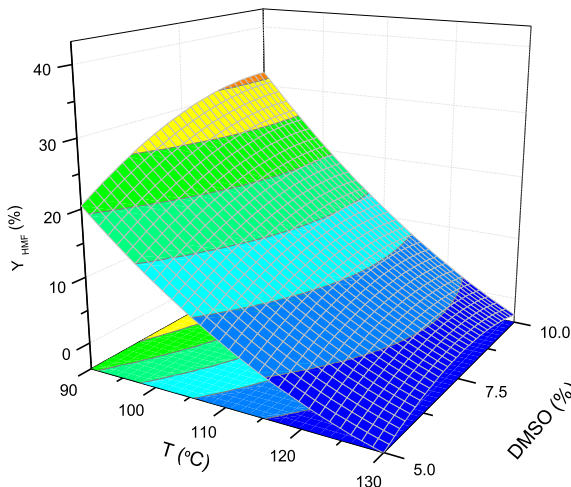
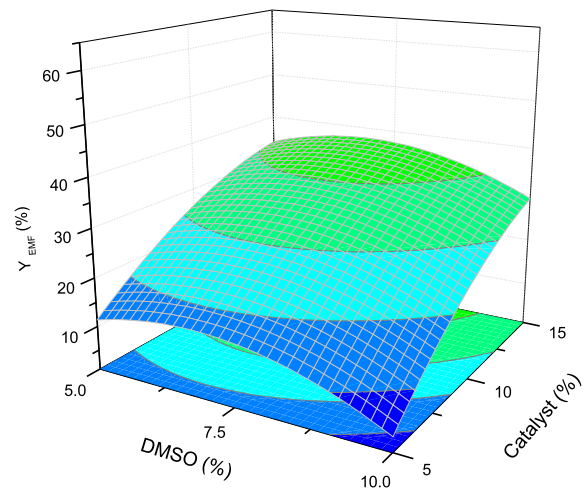
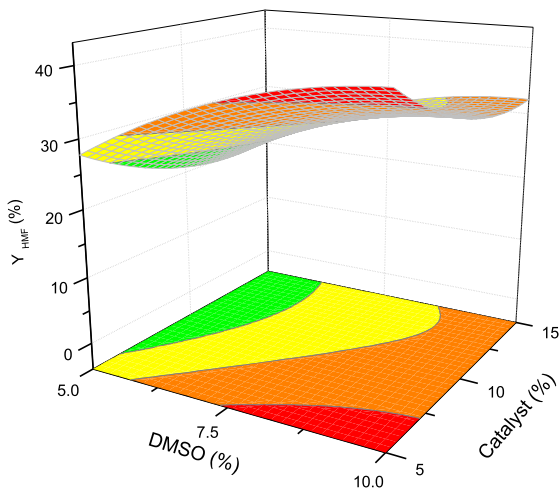
Cat = 5%**Cat = 10%****Cat = 15%**

Fig. 6. Response surfaces for yield to EMF and HMF predicted by the models for the three different levels of catalyst loading. Catalyst, Ar-SO₃H-SBA-15; time, 4 h.

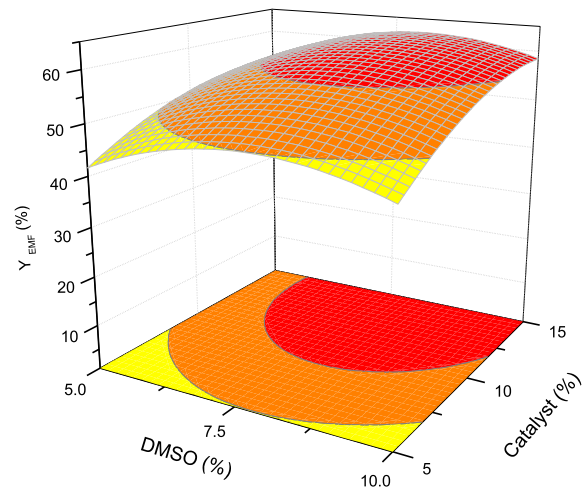
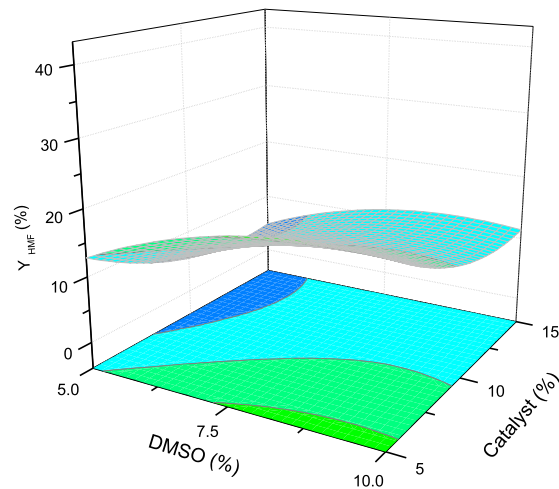
of catalyst loading has also a negative contribution. Considering both effects together, the yield to HMF can be favoured under low temperature and catalyst loading, i.e. under low reaction intensi-

ties. On the other hand, as expected from literature, DMSO displays a positive effect. An analysis of the significance of each parameter by means of Pareto chart (not shown) identified the linear contribution

T = 90°C



T = 110°C



T = 130°C

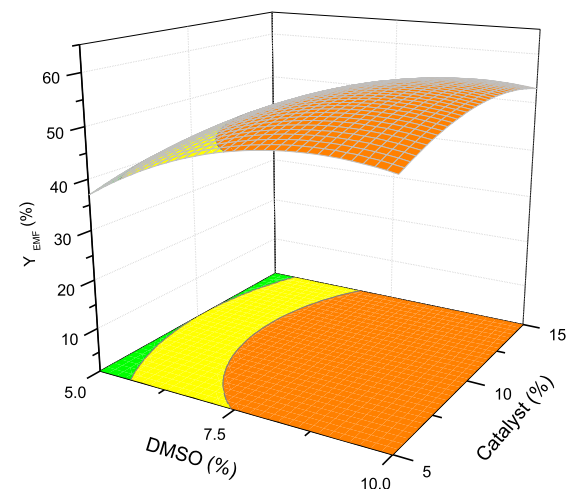
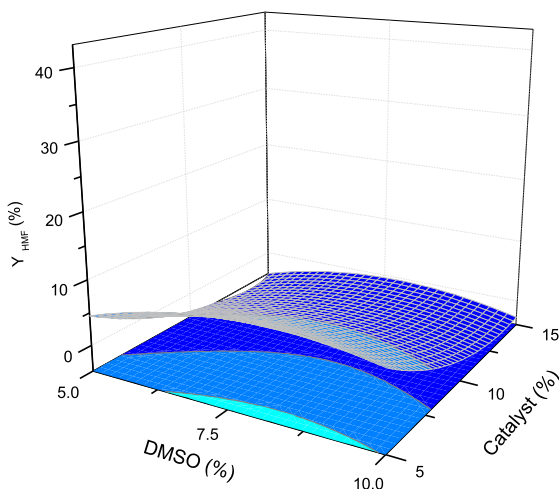


Fig. 7. Response surfaces for yield to EMF and HMF predicted by the models for the three different temperatures. Catalyst, Ar-SO₃H-SBA-15; time, 4 h.

of T as the main factor. The interactions between the three factors fall in the limit of significance. On the other hand, for the response of yield to EMF (Eq. (2)), the statistical analysis within the studied

experimental range identifies again the temperature as the most important factor, but in this case with a positive effect. However, the second factor in importance is the quadratic effect of temper-

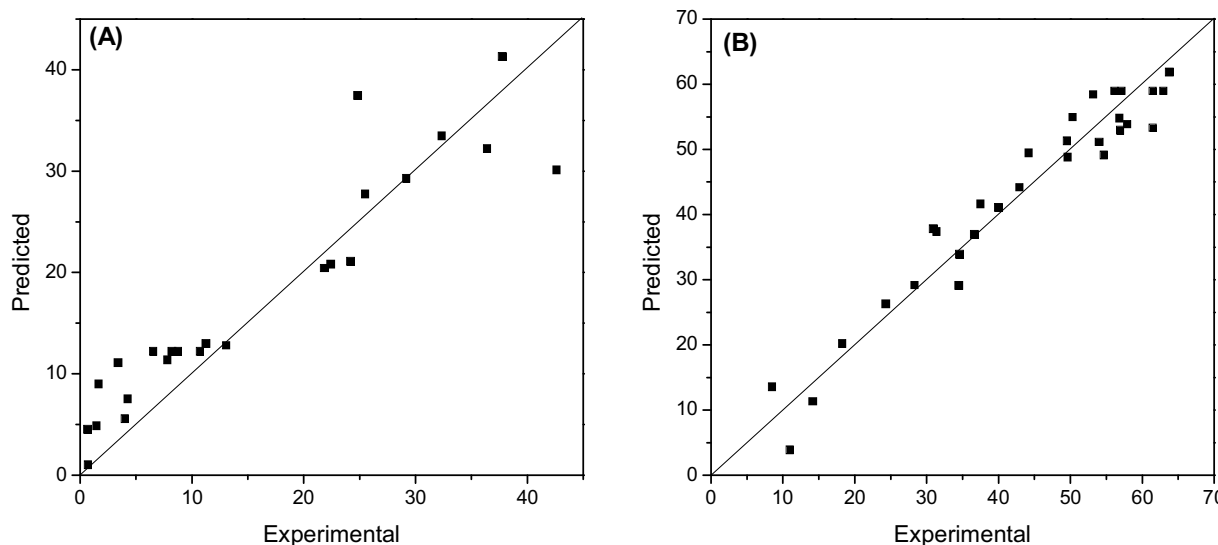


Fig. 8. Experimental versus predicted values for (A) HMF yield; (B) EMF yield. Catalyst, Ar-SBA-15; Fructose, 1 mmol; reaction time, 4 h.

ature with a negative effect. This indicates that an increase in the temperature does not produce a constant rise in Y_{EMF} , because the curvature becomes significant. Catalyst and DMSO effects appear also as positive for Y_{EMF} . Fig. 4 shows the standardized Pareto chart for this response, evidencing the significance of T and C linear contributions, as well as the quadratic effect of temperature with the three factors and the quadratic effect of DMSO. Therefore, the three factors effectively influence on the achieved yield to EMF, showing curvature of the model in the case of temperature and DMSO. This is an indication of the necessity of evaluating the factors all together in order to account for the interactions between them.

In order to facilitate the interpretation of the equations and visualize the variation of the reaction parameters, Figs. 5–7 plot the response surfaces predicted by the above technological models (Eqs. (3) and (4), Table 3) for the yields towards HMF and EMF. In Fig. 5, the surfaces of temperature-catalyst loading are depicted at the three different levels of DMSO. Fig. 6 shows the effect of temperature-DMSO for each of the fixed catalyst loadings, and Fig. 7 includes the surfaces corresponding to the variation of DMSO-catalyst loading at each temperature. As can be observed from the response surfaces, the temperature-catalyst interaction has a significant negative effect meaning that the enhancement of EMF yield with the temperature is less significant at the highest values of catalyst loading, and the corresponding improvement with the catalyst loading is also more substantial at low values of temperature. On the other hand, increasing the concentration of DMSO in the reaction medium clearly improves the yield to EMF, though a maximum can be deduced between 7.5 vol.% and 10 vol.%. Again, this confirms that in this system DMSO promotes the dehydration of fructose to HMF, subsequently etherified to EMF in the presence of ethanol. Analysing the surface responses corresponding to HMF, reverse trends can be observed leading to minimum values of Y_{HMF} when high values of Y_{EMF} are obtained.

An evaluation of the regression error was performed on the models, aiming to validate their use for making predictions. An indication of the goodness of the fit for Y_{EMF} is that the regression coefficient is over 0.93 (Table 3). The fit for Y_{HMF} , however, has a lower regression coefficient of 0.75. Fig. 8 depicts the correlation between experimental results (Table 2) and the respective predicted values obtained using the mathematical models. For the yield to EMF, there is an excellent agreement between experimental and predicted values in the whole range of values (graph on the right), while for HMF predicted values tend to be higher

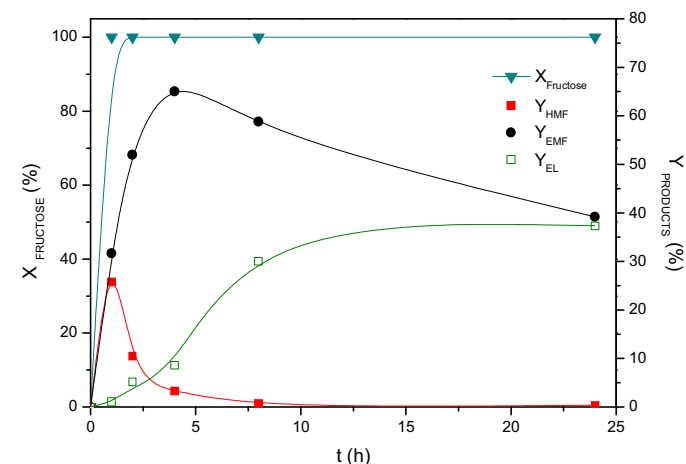


Fig. 9. Effect of reaction time in the transformation of fructose in DMSO over Ar-SO₃H-SBA-15 under the optimized reaction conditions: T = 116 °C; catalyst loading = 13.5 mol%; DMSO = 8.3 vol.%.

than experimental ones (left graph). As an additional estimation of error, the arithmetical averages and the standard deviations of both responses were calculated from the central point replicas (Table 2, runs 10–12, and 17): HMF yield (8.5 ± 1.7) and EMF yield (59.4 ± 3.3). Consequently, the obtained standard deviations are low enough to consider the experimental error, especially for the target variable yield to EMF, as not very significant.

Applying the mathematical model represented by Eq. (2), the maximal predicted value for the yield to EMF at 4 h within the experimental region is 63.4 mol%. This optimal value corresponds to the following reaction conditions: 116 °C, 13.5 mol% of catalyst loading – based on starting fructose – and 8.3 vol.% of DMSO loading ($I_T = +0.29$, $I_C = +0.70$, $I_D = +0.32$ in coded values). A catalytic experiment carried out under such reaction conditions (Fig. 9) provided the following results at 4 h: 100% X_f ; 3.3% Y_{HMF} ; 65% Y_{EMF} ; 8.9% Y_{EL} , in fair agreement with the model prediction. The kinetic curves of conversion and yields at optimized reaction conditions shown in Fig. 9 evidence that selection of reaction time is critical in order to achieve maximum yield to EMF. After reaching the maximum, around 4 h in our system, yield to EMF starts to decrease slowly insofar as the rehydration of EMF into EL takes place. Conversely, the yield to EL increases progressively with reaction time, being

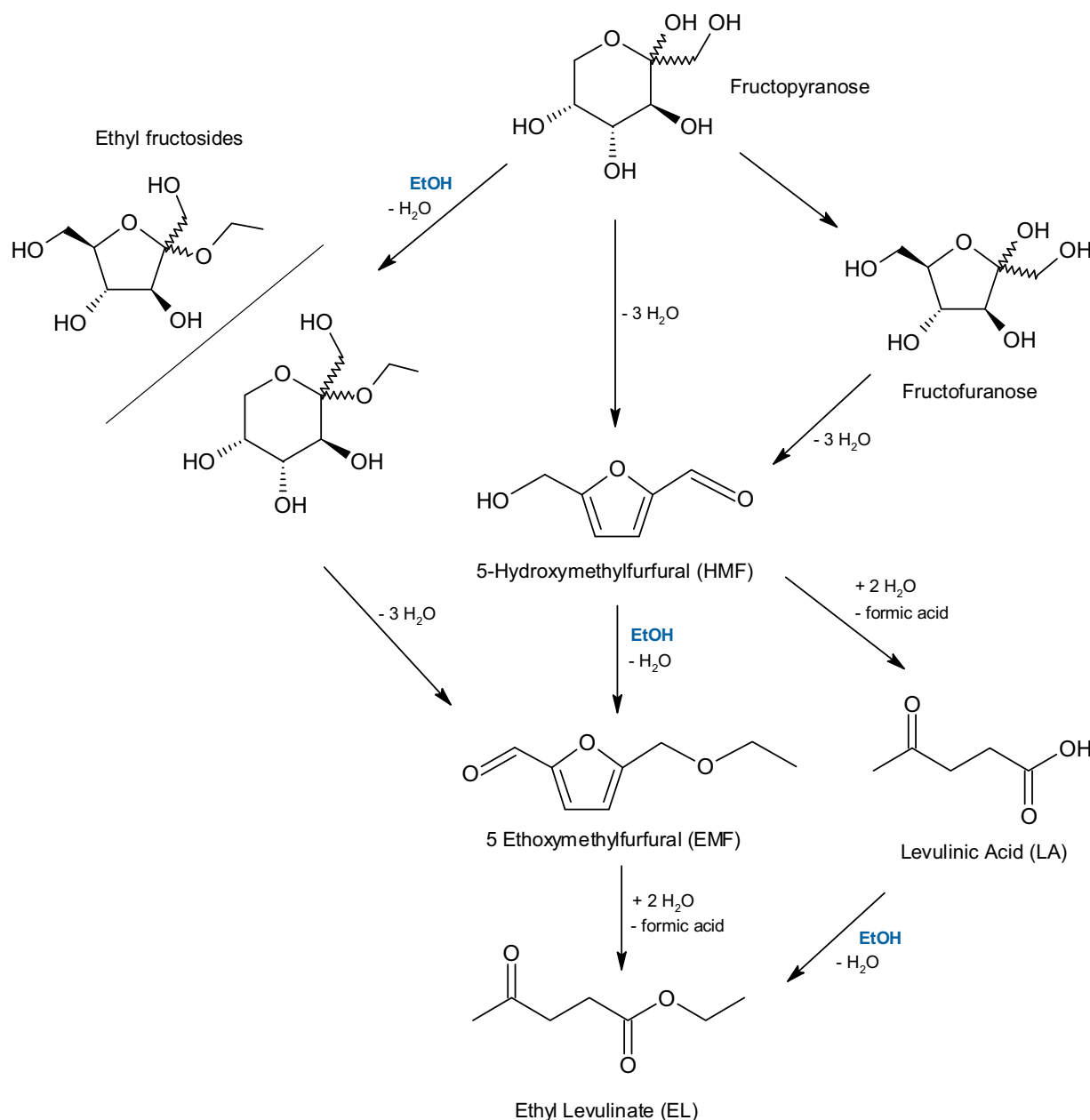


Fig. 10. Proposed reaction mechanism for the transformation of fructose in ethanol, modified from the one reported by Flannelly et al. [9].

the slowest transformation. Apparently, DMSO does not seem to prevent the rehydration of EMF into EL, as it does with the rehydration of HMF into levulinic acid [22]. This is in agreement with the mechanism proposed by Flannelly et al. [9], where EL was reported to be produced not solely from EMF, being the most feasible alternative pathway the formation of levulinic acid (via HMF) and its rapid esterification to EL with ethanol, as it has been reported for this type of catalyst at similar temperature [29]. Hence, the overall reaction mechanism would be as shown in Fig. 10, wherein a contribution to the formation of EL via levulinic acid is also considered. In such reaction network, the enhancing role of DMSO on the yield to EMF has two contributions, on the one hand, it stabilizes the furanose form of the fructose [23] and, on the other hand, it limits the rehydration of HMF into levulinic acid [22].

Additionally, aiming to evaluate the reusability of the Ar-SO₃H-SBA-15 catalyst in this reaction system, recycling tests were conducted under the optimized reaction conditions for four reac-

tion cycles. Fig. 11 displays the obtained results in terms of yields to the main products, i.e. HMF, EMF and EL (fructose conversion is total in every run). Catalyst recovery between consecutive runs was carried out by simple filtration without any further treatment. Using such a simple procedure the catalyst can be reused several times with only a small loss of activity in terms of EMF or EL production, accompanied by a small increase in the production of the precursor HMF. Noteworthy, activity loss is larger after the first reaction cycle, maintaining a more constant performance in the following cycles. Spent catalysts were analysed by means of elemental analysis, in order to evaluate the possible incorporation of organic deposits coming from undesired side reactions (humins) as well as the possible leaching of sulphur species. Elemental analysis provided almost constant sulphur content (from 2.8 to 2.7 wt%), even after 4 reaction cycles, together with an increase in carbon content (from 12.6 to 15.9 wt%). This indicates, on the one hand, the high stability of sulfonic species, which are not washed out

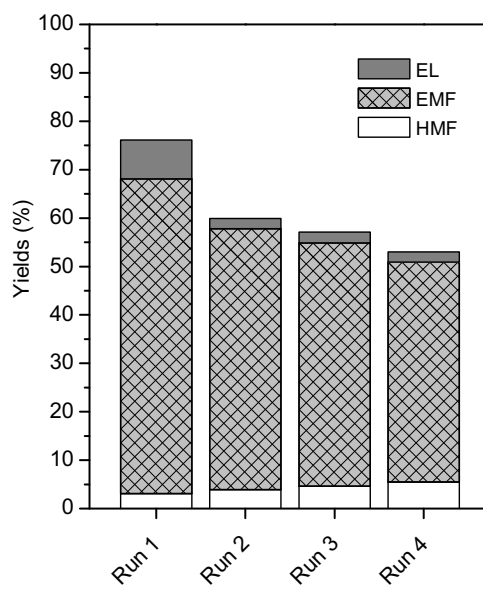


Fig. 11. Reusability of catalyst Ar-SO₃H-SBA-15 on the transformation of fructose into EMF in DMSO under the optimized conditions: T = 116 °C; catalyst loading = 13.5 mol%; DMSO = 8.3 vol.%; t = 4 h.

(leached) during the reaction, and, on the other hand, the most probable cause of deactivation, which seems to be the deposition of organic carbonaceous by-products on the catalyst's surface. Such deposits would come primarily from the formation of humins.

4. Conclusions

The use of Brønsted sulfonic acid heterogeneous catalysts allows the catalytic transformation of fructose in ethanol to give EMF and EL in high yields. Arene-sulfonic acid-modified mesoporous SBA-15 silica catalyst provides the highest yield to EMF due to the combination of excellent textural properties, acid sites surface concentration and acid strength. The use of DMSO as co-solvent in small quantities (up to 10 vol.%) clearly enhances the production of HMF and EMF. A factorial experimental design allowed for the optimization of the reaction conditions over Ar-SO₃H-SBA-15 catalyst, with the model predicting a maximum EMF yield of 63.4% at 116 °C, 13.5 mol% of catalyst loading and 8.3 vol.% of DMSO in 4 h of reaction time. A study of catalyst's reuse, without regeneration treatment, showed a slight gradual decay in activity attributed to the formation of organic deposits on the catalyst's surface.

Acknowledgements

Financial support from the Spanish Ministry of Economy and Competitiveness through the projects CTQ2011-28216-C02-01 and CTQ2014-52907-R, as well as from the Regional Government of Madrid through the project S2013-MAE-2882 is gratefully acknowledged. Likewise, we want to show our gratitude to grade students Marta Campos and Hellen Esparragoza for their collaboration in experimental tasks.

References

- [1] S.G. Wettstein, D. Martin Alonso, E. Gürbüz, J.A. Dumesic, *Curr. Opin. Chem. Eng.* 1 (2012) 218–224.
- [2] M.J. Climent, A. Corma, S. Iborra, *Green Chem.* 16 (2014) 516–547.
- [3] M. Mascal, E.B. Nikitin, *Angew. Chem. Int. Ed.* 47 (2008) 7924–7926.
- [4] G.J.M. Gruter, F. Dautzenberg, U.S. Patent Appl. 2011/0082304 A1 (2011).
- [5] P. Lanzafame, D. Temi, S. Perathoner, G. Centi, A. Macario, A. Aloise, G. Giordano, *Catal. Today* 175 (1) (2011) 435–441.
- [6] M. Mascal, E.B. Nikitin, *ChemSusChem* 2 (9) (2009) 859–861.
- [7] M. Brasholz, K. von Kanel, C.H. Hornung, S. Saubermann, J. Tsanakisidis, *Green Chem.* 13 (5) (2011) 1114–1117.
- [8] K. Barbera, P. Lanzafame, A. Pistone, S. Millesi, G. Malandrino, A. Gulino, S. Perathoner, G. Centi, *J. Catal.* 323 (2015) 19–32.
- [9] T. Flannelly, S. Dooley, J.J. Leahy, *Energy Fuels* 29 (11) (2015) 7554–7565.
- [10] D.W. Brown, A.J. Floyd, R.G. Kinsman, Y. Roshan-Ali, *J. Chem. Biotechnol.* 32 (7–12) (1982) 920–924.
- [11] M. Balakrishnan, E.R. Sacia, A.T. Bell, *Green Chem.* 14 (6) (2012) 1626–1634.
- [12] B. Liu, Z. Zhang, K. Deng, *Ind. Eng. Chem. Res.* 51 (47) (2012) 15331–15336.
- [13] G.A. Kraus, T. Guney, *Green Chem.* 14 (6) (2012) 1593–1596.
- [14] Z. Yuan, Z. Zhang, J. Zheng, J. Lin, *Fuel* 150 (2015) 236–242.
- [15] H. Li, K.S. Govind, R. Kotni, S. Shunmugavel, A. Riisager, S. Yang, *Energy Convers. Manage.* 88 (2014) 1245–1251.
- [16] H. Li, S. Saravananurugan, S. Yang, A. Riisager, *Green Chem.* (2015), <http://dx.doi.org/10.1039/C5GC01043H> (Advance Article).
- [17] B.C. Windom, T.M. Lovestead, M. Mascal, E.B. Nikitin, T.J. Bruno, *Energy Fuels* 25 (2011) 1878–1890.
- [18] Y. Roman-Leshkov, J.N. Chheda, J.A. Dumesic, *Science* 312 (2006) 1933–1937.
- [19] J.N. Chheda, Y. Roman-Leshkov, J.A. Dumesic, *Green Chem.* 9 (2007) 342–350.
- [20] R.M. Musau, R.M. Munavu, *Biomass* 13 (1987) 67–74.
- [21] Y.Y. Lee, K.C.W. Wu, *Phys. Chem. Chem. Phys.* 14 (2012) 13914–13917.
- [22] G. Morales, J.A. Melero, M. Paniagua, J. Iglesias, B. Hernández, M. Sanz, *Chin. J. Catal.* 35 (2014) 696–707.
- [23] A.S. Amarasekara, L.D. Williams, C.C. Ebene, *Carbohydr. Res.* 343 (18) (2008) 3021–3024.
- [24] H. Wang, T. Deng, Y. Wang, Y. Qi, X. Hou, Y. Zhu, *Bioresour. Technol.* 136 (2013) 394–400.
- [25] N. Rajabbeigi, R. Ranjan, M. Tsapatsis, *Microporous Mesoporous Mater.* 158 (2012) 253–256.
- [26] G. Morales, L.F. Bautista, J.A. Melero, J. Iglesias, R. Sánchez-Vázquez, *Bioresour. Technol.* 102 (2011) 9571–9578.
- [27] J.A. Melero, R. van Grieken, G. Morales, M. Paniagua, *Energy Fuel* 21 (2007) 1782–1791.
- [28] J.A. Melero, G. Vicente, G. Morales, M. Paniagua, J.M. Moreno, R. Roldan, A. Ezquerro, C. Perez, *Appl. Catal. A: Gen.* 346 (2008) 44–51.
- [29] J.A. Melero, G. Morales, J. Iglesias, M. Paniagua, B. Hernández, S. Penedo, *Appl. Catal. A: Gen.* 466 (2013) 116–122.
- [30] P.A. Russo, M.M. Antunes, P. Neves, P.V. Wiper, E. Fazio, F. Neri, F. Barreca, L. Mafra, M. Pillinger, N. Pinna, A.A. Valente, *J. Mater. Chem. A* 2 (2014) 11813–11814.
- [31] D. Margolese, J.A. Melero, S.C. Christiansen, B.F. Chmelka, G.D. Stucky, *Chem. Mater.* 12 (2000) 2448–2459.
- [32] J.A. Melero, G.D. Stucky, R. van Grieken, G. Morales, *J. Mater. Chem.* 12 (2002) 1664–1670.
- [33] J.A. Melero, R. van Grieken, G. Morales, *Chem. Rev.* 106 (2006) 3790–3812.
- [34] G. Morales, G. Athens, B.F. Chmelka, R. van Grieken, J.A. Melero, *J. Catal.* 254 (2008) 205–217.
- [35] G.E.P. Box, W.G. Hunter, J.S. Hunter, *Statistics for Experiments, an Introduction to Design, Data Analysis and Model Building*, Wiley, New York, 1978.